# DETECTION OF THE SECOND R-PROCESS PEAK ELEMENT TELLURIUM IN METAL-POOR STARS[1][,2]

Ian U. Roederer,[3] James E. Lawler,[4] John J. Cowan,[5] Timothy C. Beers,[6,7,8] Anna Frebel,[9] Inese I. Ivans,[10]
Hendrik Schatz,[7,8,11] Jennifer S. Sobeck,[12] Christopher Sneden[13]

*Accepted for publication in the Astrophysical Journal Letters*

## ABSTRACT

Using near-ultraviolet spectra obtained with the Space Telescope Imaging Spectrograph onboard the *Hubble Space Telescope*, we detect neutral tellurium in three metal-poor stars enriched by products of $r$-process nucleosynthesis, BD +17 3248, HD 108317, and HD 128279. Tellurium (Te, $Z = 52$) is found at the second $r$-process peak ($A \approx 130$) associated with the $N = 82$ neutron shell closure, and it has not been detected previously in Galactic halo stars. The derived tellurium abundances match the scaled Solar System $r$-process distribution within the uncertainties, confirming the predicted second peak $r$-process residuals. These results suggest that tellurium is predominantly produced in the main component of the $r$-process, along with the rare earth elements.

*Subject headings:* nuclear reactions, nucleosynthesis, abundances — stars: abundances — stars: individual (BD +17 3248, HD 108317, HD 128279) — stars: Population II

## 1. INTRODUCTION

In the quest to understand the production of the heaviest elements in the universe, several invaluable datasets for testing nucleosynthesis models are available, including the isotopic and elemental abundance patterns found in meteorites, the Solar photosphere, and metal-poor halo stars. All elements heavier than the iron group are produced (at least in part) by neutron-capture reactions. These reactions occur on timescales that are slow or rapid, relative to the average $\beta$-decay timescales of unstable nuclei along the reaction chain, and thus they are known as the $s$-process and $r$-process, respectively.

The Solar System (S.S.) $r$-process distribution is calculated as the "residual" in the S.S. isotopic abundance distribution after subtracting the predicted $s$-process distribution from the total abundances. This may be calculated analytically (e.g., Seeger et al. 1965; Cameron 1982; Käppeler et al. 1989) or via simulations that rely on stellar evolution models and nuclear reaction networks (e.g., Arlandini et al. 1999; Bisterzo et al. 2011). Nuclei with neutron numbers $N = 50$, 82, and 126 have reduced neutron-capture cross sections, giving rise to "peaks" in the abundance distributions. Models that capture the essential physics of these processes must be able to reproduce the nucleosynthetic yields, and the neutron-capture peaks are highly sensitive probes of this physics.

The third $r$-process peak elements osmium through platinum ($76 \leq Z \leq 78$; $A \approx 195$) are associated with the $N = 126$ shell closure. Their strongest absorption lines in stellar spectra are found in the near-ultraviolet (NUV) and cannot be observed from ground-based facilities. Using spectra obtained with the Goddard High Resolution Spectrograph onboard the *Hubble Space Telescope* (*HST*), Cowan et al. (1996) and Sneden et al. (1998) reported the first detections of these elements in metal-poor stars enriched by the $r$-process. The osmium and platinum abundances were consistent with the scaled S.S. $r$-process distribution. This result established the similarity of the predicted S.S. $r$-process distribution and the $r$-process distribution in halo stars that formed many Gyr before the condensation of the Solar nebula. Subsequent detections of osmium and platinum in additional halo stars using the Space Telescope Imaging Spectrograph (STIS) onboard *HST* by Cowan et al. (2002, 2005), Sneden et al. (2003), Roederer et al. (2010b), and Barbuy et al. (2011) have reaffirmed this similarity.

Absorption lines of the second $r$-process peak elements tellurium, iodine, and xenon ($52 \leq Z \leq 54$; $A \approx 130$), associated with the $N = 82$ shell closure, are not observable from the ground in halo stars. Transitions from the ground state of iodine and xenon all occur at wavelengths shorter than $2000\,\text{Å}$ (e.g., Morton 2000). Tellurium has not been detected in the Solar photosphere, and its S.S. abundance is known only from studies of meteorites (e.g., Anders & Ebihara 1982). Predictions suggest that

[1] Based on observations made with the NASA/ESA Hubble Space Telescope, obtained at the Space Telescope Science Institute, which is operated by the Association of Universities for Research in Astronomy, Inc., under NASA contract NAS 5-26555. These observations are associated with programs GO-8342 and GO-12268.

[2] Some of the data presented in this paper were obtained from the Multimission Archive at the Space Telescope Science Institute (MAST). STScI is operated by the Association of Universities for Research in Astronomy, Inc., under NASA contract NAS5-26555. These data are associated with programs GO-7348, GO-7402, GO-8197, and GO-9455.

[3] Carnegie Observatories, Pasadena, CA 91101, USA

[4] Department of Physics, University of Wisconsin, Madison, WI 53706, USA

[5] Homer L. Dodge Department of Physics and Astronomy, University of Oklahoma, Norman, OK 73019, USA

[6] National Optical Astronomy Observatory, Tucson, AZ 85719, USA

[7] Department of Physics & Astronomy, Michigan State University, E. Lansing, MI 48824, USA

[8] Joint Institute for Nuclear Astrophysics, Michigan State University, E. Lansing, MI 48824, USA

[9] Massachusetts Institute of Technology, Kavli Institute for Astrophysics and Space Research, Cambridge, MA 02139, USA

[10] Department of Physics and Astronomy, University of Utah, Salt Lake City, UT 84112, USA

[11] National Superconducting Cyclotron Laboratory, Michigan State University, East Lansing, MI 48824, USA

[12] Department of Astronomy & Astrophysics, University of Chicago, Chicago, IL 60637, USA

[13] Department of Astronomy, University of Texas at Austin, Austin, TX 78712, USA

TABLE 1
Atomic Transition Probabilities for Te i

| Wavenumber (cm$^{-1}$) | $\lambda_{air}$ (Å) | E$_{upper}$ (cm$^{-1}$) | $J_{upper}$ | E$_{lower}$ (cm$^{-1}$) | $J_{lower}$ | Transition Probability (10$^6$ s$^{-1}$) | log($gf$) |
|---|---|---|---|---|---|---|---|
| 46652.738 | 2142.8218 | 46652.738 | 1 | 0.000 | 2 | 231(37) | $-0.32$ |
| 41946.238 | 2383.2772 | 46652.738 | 1 | 4706.500 | 0 | 30(5) | $-1.11$ |
| 41902.026 | 2385.7920 | 46652.738 | 1 | 4750.712 | 1 | 60(10) | $-0.81$ |
| 36094.861 | 2769.6596 | 46652.738 | 1 | 10557.877 | 2 | 0.90(0.15) | $-2.51$ |

$\approx$ 17–20% of the tellurium in the S.S. originated in the $s$-process, while the remainder was presumably produced by the $r$-process (e.g., Sneden et al. 2008; Bisterzo et al. 2011). Contributions from charged-particle reactions (i.e., proton captures) to tellurium isotopes are expected to be minimal (e.g., Käppeler et al. 1989). We are aware of three previous detections of tellurium beyond the S.S.: a single, blended line in the F-type main sequence star Procyon (Yushchenko & Gopka 1996); the $s$-process rich planetary nebula IC 418 (Sharpee et al. 2007); and the chemically peculiar star HD 65949 (Cowley et al. 2010), which is not ideal for detailed exploration of the $s$- or $r$-process patterns due to the chemical stratification that occurs in its warm atmosphere.

The tellurium abundance in metal-poor halo stars offers an independent check on the predicted $r$-process abundance of tellurium in the S.S. It also constrains the conditions of the $r$-process operating early in the Galaxy. In this Letter we report the detection of an absorption line of Te i at 2385 Å in the atmospheres of three $r$-process enriched stars observed with STIS. We combine the abundances derived from this line with abundances of other heavy elements derived from both space- and ground-based data to form a more complete $r$-process abundance distribution.

## 2. OBSERVATIONS

In Program GO-12268, we have used STIS (Kimble et al. 1998; Woodgate et al. 1998) to obtain new spectra of 4 metal-poor stars with modest or sub-solar levels of $r$-process enrichment. The spectra of two of these stars, HD 108317 and HD 128279, are useful for abundance work at 2385 Å. These data were taken using the E230M echelle grating and the NUV Multianode Microchannel Array (MAMA) detector, yielding a spectral resolution (R $\equiv$ $\lambda/\Delta\lambda$) $\sim$ 30,000 and wavelength coverage from 2280–3115 Å. Standard reduction and calibration procedures were used; see Roederer et al. (2012) for details. We also examine previous STIS observations obtained in Program GO-8342 (Cowan et al. 2002) of the metal-poor $r$-process rich standard star BD +17 3248. The signal-to-noise ratios in the continuum near 2385 Å are $\sim$ 100/1 for HD 108317 and HD 128279 and slightly less in BD +17 3248.

## 3. THE TE I 2385 Å ABSORPTION LINE

HD 108317 and HD 128279 have nearly identical stellar parameters and metallicities (Section 4), but the heavy elements in HD 108317 are enhanced by a factor of $\sim$ 2–3 relative to HD 128279. In these two stars, most differences in the NUV spectral region can be traced to absorption by elements heavier than the iron group. One such difference is observed at 2385.8 Å,

where the absorption in HD 108317 is stronger than in HD 128279. We have searched the National Institute of Standards and Technology (NIST) Atomic Spectra Database (Ralchenko et al. 2011), the Kurucz & Bell (1995) line lists, and the Morton (2000) compilation of low excitation transitions of heavy elements to identify the species responsible for this absorption. These sources indicate that the only probable transition is Te i 2385.79 Å. The first ionization potential of tellurium is high (9.01 eV), so a substantial amount of neutral tellurium ($\sim$ 50%) is present.

We calculate transition probabilities of four Te i transitions sharing the same upper level as the 2385.79 Å transition. These values are listed in Table 1. We adopt energy levels from Morillon & Vergès (1975), branching ratios from Ubelis & Berzinsh (1983), and the laser-induced fluorescence lifetime measurement of the upper level from Bengtsson et al. (1992). The log($gf$) values have an uncertainty of about 16%, where the largest source of uncertainty arises from the lifetime measurement.

Other relatively strong transitions of Te i should lie at 2142.82 Å and 2383.28 Å. Detecting either of these features would strongly confirm our Te i detection based on the 2385.79 Å transition. Unfortunately, the 2383.28 Å transition is buried within an absorption feature (EW > 0.5 Å) dominated by the Fe ii line at 2383.25 Å, and it is not useful for this purpose. The 2142.82 Å transition is not covered in our data. In the STIS archives we find high-resolution spectra of two metal-poor stars, HD 94028 and HD 140283, that cover both the 2142 Å and 2385 Å lines. Both stars are warmer than those in our sample (e.g., Peterson 2011), so the fraction of tellurium present in the neutral state in these stars is lower. No absorption is detected at 2385.79 Å in HD 140283, but a very weak feature is detected in HD 94028. In HD 94028, the Te i feature predicted at 2142.82 Å is blended with an absorption feature at 2142.83 Å that may be due to Fe i. Our syntheses suggest that some of the absorption may be due to Te i, but it is impossible to derive a reliable abundance from it. We are unable to substantiate our detection with additional Te i lines, so we proceed with caution.

## 4. ABUNDANCE ANALYSIS

We perform a standard abundance analysis, using synthesis techniques, to derive the tellurium abundance; see Roederer et al. (2012) for details. We use models interpolated from the $\alpha$-enhanced ATLAS9 grid (Castelli & Kurucz 2004), and we perform the analysis using the latest version of the analysis code MOOG (Sneden 1973) under the assumption that local thermo-
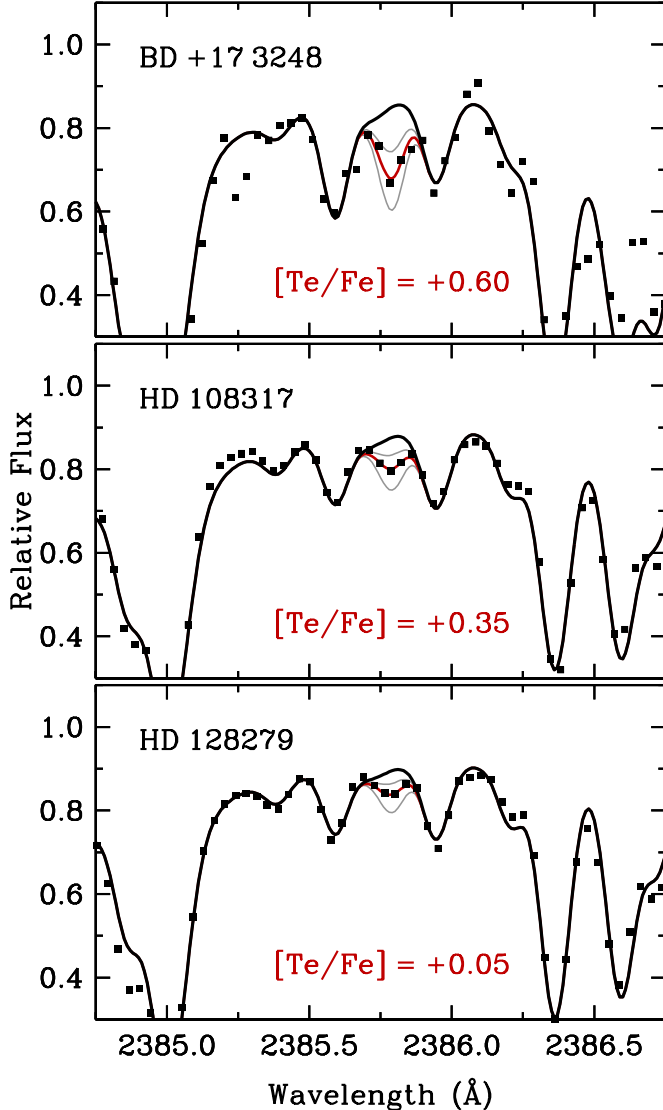
FIG. 1.— Comparison of observed and synthetic spectra around the Te I 2385 Å line. The bold red line represents the best-fit abundance, the thin gray lines represent variations in this abundance by ± 0.30 dex, and the bold black line represents a synthesis with no tellurium.
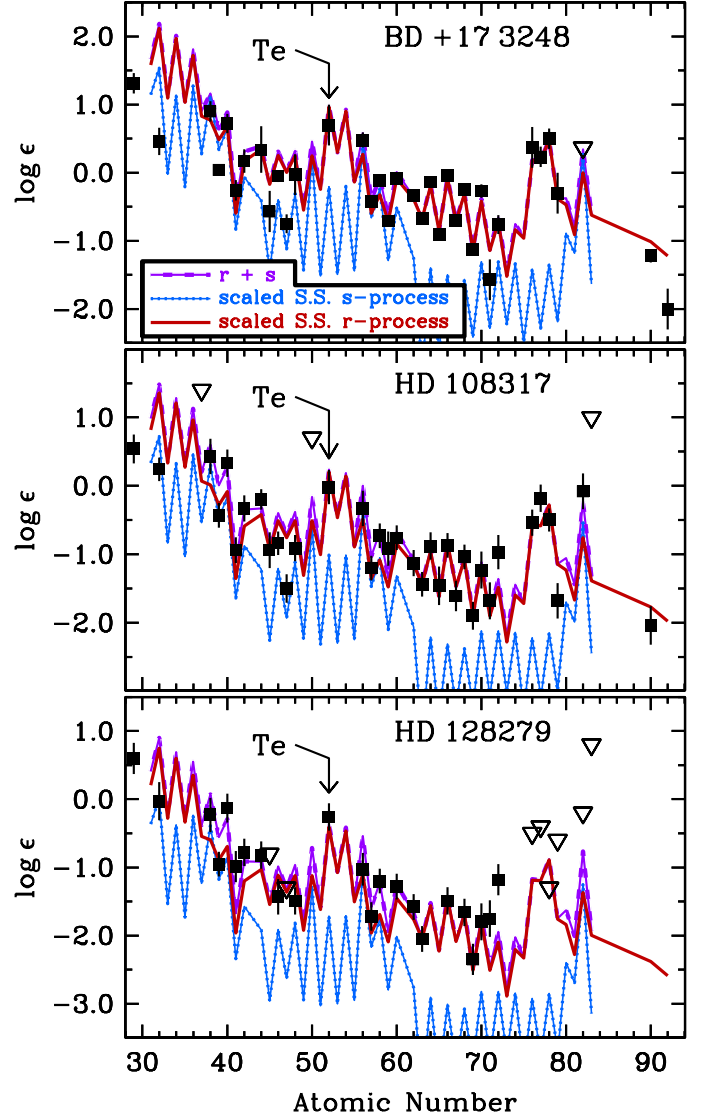
FIG. 2.— Logarithmic abundances in BD +17 3248, HD 108317, and HD 128279. Filled squares indicate detections, and open downward facing triangles indicate upper limits. Two curves (blue and red) represent the scaled S.S. s- and r-process abundances from Sneden et al. (2008); the "strong" s-process component contributions to lead and bismuth are taken from Bisterzo et al. (2011). The third curve (purple) represents a combined r + s distribution. The r-process and r + s distributions are normalized to the europium (Eu, $Z = 63$) abundance of each star, and the s-process distributions are normalized to barium (Ba, $Z = 56$). The tellurium abundances are derived in the present study. References for the other abundances are given in the text.

dynamic equilibrium (LTE) governs the the excitation and ionization. Our model parameters for BD +17 3248, HD 108317, and HD 128279 are, respectively, $T_{\rm eff}/\log g/[{\rm M/H}]/v_{\rm t} = 5200$ K/1.80/−2.08/1.90 km s$^{-1}$ (Cowan et al. 2002), 5100 K/2.67/−2.37/1.50 km s$^{-1}$, and 5080 K/2.57/−2.49/1.60 km s$^{-1}$ (Roederer et al. 2012).

In the spectral region surrounding the Te I 2385 Å line (± 10 Å), our syntheses predict absorption from other species at approximately 95% of the wavelengths where a line is observed. This agreement is reassuring. Often the transition probabilities must be adjusted to reproduce the observed spectrum, but this is a well-known problem in the UV (e.g., Leckrone et al. 1999).

Our syntheses suggest that the Te I line at 2385.79 Å is in a relatively clean spectral window, as shown in Fig-

ure 1. Strong Fe II lines at 2383.04 Å and 2388.63 Å depress the continuum by 10–20%, which introduces additional uncertainty into the derived tellurium abundance. We can fit weaker Fe I lines at 2385.59 Å and 2385.94 Å that mildly affect the observed Te I line profile. Our syntheses suggest that a Cr I transition at 2385.72 Å contributes a small amount of absorption to the observed line profile. NIST quotes an uncertainty of 40% for this $\log(gf)$ value, and we produce an acceptable fit to the overall line profile by varying its strength accordingly. We estimate errors by accounting for uncertainties in the model atmosphere parameters, $\log(gf)$ values, and

the fit to the observed line profile (Cowan et al. 2005; Roederer et al. 2012). Zero-point uncertainties may exist in abundance ratios of elements derived from species of different ionization states. We caution that such ratios (e.g., [Te/Zr], [Te/Ba], [Te/Eu]) are less secure than ratios derived from species in the same ionization state (e.g., [Te/Pd], [Te/Pt], [Ba/Eu]).

We derive tellurium abundances ($\log \epsilon$) from the 2385 Å line in BD +17 3248, HD 108317, and HD 128279 of $+0.70 \pm 0.30$, $-0.02 \pm 0.25$, and $-0.26 \pm 0.25$, respectively. Referencing these abundances to the iron abundance derived from Fe I in each star ([Fe/H] = $-2.08$, $-2.55$, $-2.49$, respectively) and the S.S. meteoritic abundance of tellurium ($\log \epsilon = +2.18$; Asplund et al. 2009), we calculate [Te/Fe] = $+0.60$, $+0.35$, and $+0.05$, respectively.

## 5. DISCUSSION

These stars are rich laboratories to study the nucleosynthesis of heavy elements. When the new tellurium abundances are combined with previous abundance determinations in BD +17 3248, HD 108317, and HD 128279 (Cowan et al. 2002, 2005; Sneden et al. 2009; Roederer et al. 2009, 2010b, 2012), a total of 34, 34, and 22 elements heavier than zinc ($Z = 30$) have been detected in the atmospheres of these stars.

Figure 2 illustrates the heavy element distributions in BD +17 3248, HD 108317, and HD 128279. The scaled S.S. $s$- and $r$-process abundance patterns are shown for comparison (Sneden et al. 2008; Bisterzo et al. 2011). The $r$-process residuals implicitly include contributions from all heavy element nucleosynthesis mechanisms other than the $s$-process; e.g., a light element primary process (LEPP; Travaglio et al. 2004). The stellar abundance patterns—including the new tellurium abundances—conform more closely to the scaled S.S. $r$-process pattern than to the scaled S.S. $s$-process pattern, as noted previously (e.g., Cowan et al. 2002; Roederer et al. 2010a).

A small $s$-process contamination, indicated by the combined $r + s$ distribution in Figure 2, might improve the fit to several elements in HD 108317. In S.S. material a substantial portion of these elements (e.g., strontium, zirconium, cerium, lead; $Z = 38, 40, 58, 82$) is attributed to the $s$-process, so it is not surprising that they are the first to show evidence of $s$-process enrichment. There is no clear evidence of $s$-process contamination in BD +17 3248. There is conflicting evidence of $s$-process contamination in HD 128279; the fit to several elements is improved by including an $s$-process component (e.g., strontium, zirconium, cerium), while for others (e.g., barium) it is not. Furthermore, HD 128279 is a probable member of a stellar stream, and abundances in the other members suggest that the star-forming regions of the stream's progenitor system were not polluted by significant amounts of $s$-process material (Roederer et al. 2010a). We advise against using these combined $r + s$ distributions to quantify the relative amount of $s$- and $r$-process material present. The predicted S.S. distributions are the cumulative yields of many nucleosynthesis events and may not be representative of individual $s$- or $r$-process events. We conclude that $r$-process nucleosynthesis is mainly responsible for the heavy elements in these stars.

Despite the possibility of a small amount of $s$-process

contamination, several features are clear from Figure 2. The $s$-process contamination has a negligible effect on the second and third $r$-process peaks and the heavy end of the rare earth domain. The more pronounced odd-even effect observed in the stellar distributions for strontium through cadmium, though mitigated by assuming an $s$-process contribution, persists. One platinum ($Z = 78$) non-detection in HD 128279 by Roederer et al. (2012) indicates that platinum falls below the scaled S.S. $r$-process prediction, so the third $r$-process peak elements may be slightly deficient in this star. Otherwise, these patterns are remarkably constant considering that the $r$-process enrichment (e.g., [Eu/Fe]) spans 1 dex in the three stars.

These results confirm that the tellurium abundances in halo stars match the predicted S.S. $r$-process residuals for the second $r$-process peak. They also indicate that tellurium is predominantly produced, along with the rare earth elements, in the main component of the $r$-process, as has been predicted (e.g., Kratz et al. 2007; Farouqi et al. 2010). The ratio of second-to-third $r$-process peak abundances is an important benchmark for $r$-process models, and our results confirm that the $r$-process operating in the early Galaxy produced ratios like those of the predicted S.S. $r$-process residuals. The S.S. and halo star abundances of elements lighter than tellurium have revealed the presence of material from additional nucleosynthesis mechanisms (e.g., Wasserburg et al. 1996; Travaglio et al. 2004; Qian & Wasserburg 2008) and possibly variations in the physical conditions of $r$-process nucleosynthesis (e.g., Truran et al. 2002; Roederer et al. 2010c). Our results suggest that contributions from other nucleosynthesis mechanisms to the tellurium in these stars are minor.

Tellurium is the heaviest element whose $r$-process production can be calculated largely based on experimental nuclear data (Dillmann et al. 2003). Selenium, which has not been detected in $r$-process enriched metal-poor stars, is another. These are the first observations of tellurium produced by the $r$-process operating in the early Galaxy, and they provide critical data for validating $r$-process models with the least amount of nuclear physics uncertainty.

*Facilities:* HST (STIS)

## REFERENCES

Anders, E., & Ebihara, M. 1982, Geochim. Cosmochim. Acta, 46, 2363

Arlandini, C., Käppeler, F., Wisshak, K., et al. 1999, ApJ, 525, 886

Asplund, M., Grevesse, N., Sauval, A. J., & Scott, P. 2009, ARA&A, 47, 481

Barbuy, B., Spite, M., Hill, V., et al. 2011, A&A, 534, A60

Bengtsson, G. J., Berzinsh, U., Larsson, J., & Svanberg, S. 1992, Zeitschrift fur Physik D Atoms Molecules Clusters, 23, 29

Bisterzo, S., Gallino, R., Straniero, O., Cristallo, S., & Käppeler, F. 2011, MNRAS, 418, 284

Cameron, A. G. W. 1982, Ap&SS, 82 123

Castelli, F., & Kurucz, R. L. Proc. IAU Symp. No 210, Modelling of Stellar Atmospheres, eds. N. Piskunov et al. 2003, A20

Cowan, J. J., Sneden, C., Truran, J. W., & Burris, D. L. 1996, ApJ, 460, L115

Cowan, J. J., Sneden, C., Burles, S., et al. 2002, ApJ, 572, 861

Cowan, J. J., Sneden, C., Beers, T. C., et al. 2005, ApJ, 627, 238

Cowley, C. R., Hubrig, S., Palmeri, P., et al. 2010, MNRAS, 405, 1271

Dillmann, I., Kratz, K.-L., Wöhr, A., et al. 2003, Physical Review Letters, 91, 162503

Farouqi, K., Kratz, K.-L., Pfeiffer, B., et al. 2010, ApJ, 712, 1359

Käppeler, F., Beer, H., & Wisshak, K. 1989, Reports on Progress in Physics, 52, 945

Kimble, R. A., Woodgate, B. E., Bowers, C. W., et al. 1998, ApJ, 492, L83

Kratz, K.-L., Farouqi, K., Pfeiffer, B., et al. 2007, ApJ, 662, 39

Kurucz, R. L., & Bell, B. 1995, Kurucz CD-ROM, Cambridge, MA: Smithsonian Astrophysical Observatory

Leckrone, D. S., Proffitt, C. R., Wahlgren, G. M., Johansson, S. G., & Brage, T. 1999, AJ, 117, 1454

Morillon, C., & Vergès, J. 1975, Phys. Scr, 12, 129

Morton, D. C. 2000, ApJS, 130, 403

Peterson, R. C. 2011, ApJ, 742, 21

Qian, Y.-Z., & Wasserburg, G. J. 2008, ApJ, 687, 272

Ralchenko, Yu., Kramida, A., Reader, J., et al. 2011, NIST Atomic Spectra Database, version 4.1, available online: http://physics.nist.gov/asd

Roederer, I. U., Kratz, K.-L., Frebel, A., et al. 2009, ApJ, 698, 1963

Roederer, I. U., Sneden, C., Thompson, I. B., Preston, G. W., & Shectman, S. A. 2010a, ApJ, 711, 573

Roederer, I. U., Sneden, C., Lawler, J. E., & Cowan, J. J. 2010b, ApJ, 714, L123

Roederer, I. U., Cowan, J. J., Karakas, A. I., et al. 2010c, ApJ, 724, 975

Roederer, I. U., Lawler, J. E., Sobeck, J. S., et al. 2012, ApJS, submitted

Seeger, P. A., Fowler, W. A., & Clayton, D. D. 1965, ApJS, 11, 121

Sharpee, B., Zhang, Y., Williams, R., et al. 2007, ApJ, 659, 1265

Sneden, C. A. 1973, Ph.D. Thesis, Univ. of Texas at Austin

Sneden, C., Cowan, J. J., Burris, D. L., & Truran, J. W. 1998, ApJ, 496, 235

Sneden, C., Cowan, J. J., Lawler, J. E., et al. 2003, ApJ, 591, 936

Sneden, C., Cowan, J. J., & Gallino, R. 2008, ARA&A, 46, 241

Sneden, C., Lawler, J. E., Cowan, J. J., Ivans, I. I., & Den Hartog, E. A. 2009, ApJS, 182, 80

Travaglio, C., Gallino, R., Arnone, E., et al. 2004, ApJ, 601, 864

Truran, J. W., Cowan, J. J., Pilachowski, C. A., & Sneden, C. 2002, PASP, 114, 1293

Ubelis, A. P., & Berzinsh, U. V. 1983, Phys. Scr, 28, 171

Wasserburg, G. J., Busso, M., & Gallino, R. 1996, ApJ, 466, L109

Woodgate, B. E., Kimble, R. A., Bowers, C. W., et al. 1998, PASP, 110, 1183

Yushchenko, A. V., & Gopka, V. F. 1996, Astronomical and Astrophysical Transactions, 10, 307